Article

A Search for Heterocycles in GOTHAM Observations of TMC-1

Published as part of The Journal of Physical Chemistry virtual special issue "10 Years of the ACS PHYS Astrochemistry Subdivision".

Timothy J. Barnum,* Mark A. Siebert, Kin Long Kelvin Lee, Ryan A. Loomis, P. Bryan Changala, Steven B. Charnley, Madelyn L. Sita, Ci Xue, Anthony J. Remijan, Andrew M. Burkhardt, Brett A. McGuire,* and Ilsa R. Cooke*

ACCESS | 📊 Metrics & More | 📖 Article Recommendations | 🔵 Supporting Information

ABSTRACT: We have conducted an extensive search for nitrogen-, oxygen-, and sulfur-bearing heterocycles toward Taurus Molecular Cloud 1 (TMC-1) using the deep, broadband centimeter-wavelength spectral line survey of the region from the GOTHAM large project on the Green Bank Telescope. Despite their ubiquity in terrestrial chemistry, and the confirmed presence of a number of cyclic and polycyclic hydrocarbon species in the source, we find no evidence for the presence of any heterocyclic species. Here, we report the derived upper limits on the column densities of these molecules obtained by Markov Chain Monte Carlo (MCMC) analysis and compare this approach to traditional single-line upper limit measurements. We further hypothesize why these molecules are absent in our data, how they might form in interstellar space, and the nature of observations that would be needed to secure their detection.
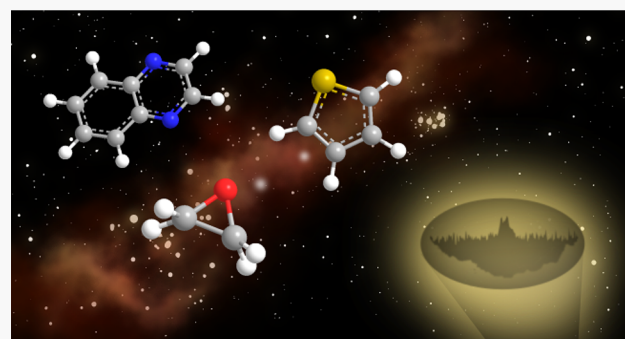
INTRODUCTION

Aromatic compounds are an important class of molecules of astrophysical and astrobiological interest. In particular, polycyclic aromatic hydrocarbons (PAHs) are abundant in interstellar and circumstellar environments, and it has been estimated that as much as 25% of all interstellar carbon is sequestered in these species.[1] Despite their significance to terrestrial chemistry, individual five- and six-membered aromatic rings, as well as PAHs, have only recently been identified in the interstellar medium (ISM).[2−9]

Heterocycles are a related class of cyclic molecules with atoms of at least two different elements as members of its ring(s). In general, a CH unit in a carbon ring is replaced by a heavier heteroatom, such as N, O, or S. Among these, N-heterocycles are of great biological significance as they form the backbone of nucleobases, that is, subunits of the DNA and RNA that carry the genetic information in living systems.

The astrophysical relevance of heterocycles has been appreciated since the discovery of N-, O-, and S-heterocycles in carbonaceous chondrites.[10] For example, a number of S-heterocycles have been detected in the Yamato-791198 meteorite,[11] while N-heterocycles including pyridines, pyrimidines, quinolines, and isoquinolines have been detected in several chondrites, including Orgueil,[12] Murchison,[13−16] and Murray.[17] Their extraterrestrial origins have been confirmed by isotopic studies,[18] but it remains difficult to ascertain their chemical origin.[19]

Following the recent detection of benzonitrile (c-C_6H_5CN) in the quiescent molecular cloud Taurus Molecular Cloud 1 (TMC-1),[2] both five-membered and bicyclic nitrile species (hydrocarbons with a cyanide [−CN] functional group) have been detected using our GOTHAM line survey[3−6] and the QUIJOTE survey of Cernicharo and colleagues.[7−9] Benzonitrile has also been observed in four additional molecular clouds in different stages of prestellar evolution, suggesting that aromatic molecules are ubiquitous in interstellar environments.[20]
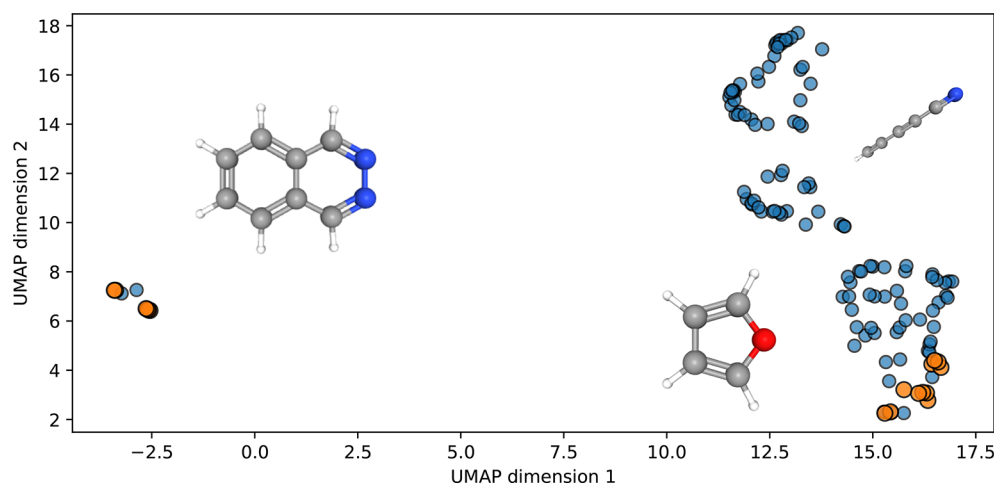
While these detections have shown that aromatic molecules are prevalent in TMC-1, these molecules are either pure aromatic hydrocarbons or functionalized aromatics with a −CN or C_2H group in the place of a hydrogen on the ring. With the detection of several aromatics now secure, heterocyclic molecules are the next logical step in chemical
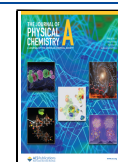
Figure 1. Visualizations of a two-dimensional projection of the chemical embedding space spanned by the current chemical inventory of TMC-1 (blue) and of the proposed heterocyclic species (orange). Representative structures of indicative molecules annotate how chemical complexity in this source is traversed and divided: molecules such as the cyanopolyynes extend from the top to the bottom on the right, connecting with single-ring heterocycles such as furan toward the bottom. On the left, two-ring species such as cyanonaphthalene (not pictured) and their heterocyclic analogues.

complexity to explore. Yet, to date, no five- or six-membered ring heterocycles have been detected in TMC-1 nor in any region of interstellar space.[21] For these relatively large molecules, the number of possible isomers renders prioritization difficult, and thus we choose to combine conventional chemical intuition and recent machine learning work by Lee et al.[22]

To illustrate how machine learning can be used to guide astrochemical studies, Figure 1 represents a "chemical map", where the abscissa and ordinate represent the 2D space that comprises molecules found in TMC-1 and those studied in the present work. The absolute values are not important; however, the relative distance between points (i.e., molecules) corresponds with chemical similarity. To briefly summarize the technique, the Uniform Manifold Approximation and Projection (UMAP) method[23] is an unsupervised algorithm that learns an approximate mapping between high-dimensional data—in this case, a 128-dimensional chemical embedding obtained through natural language models[22,24]—to lower dimensionality while preserving the topology of the original manifold as faithfully as possible. The target species comprise two frontiers: monocyclic (lower right of Figure 1) and bicyclic (left of Figure 1) rings, which are currently sparsely represented and for that reason, are among the most informative to quantify in TMC-1. By constraining the abundance of these species, we are able to effectively and precisely place boundary conditions on one edge of chemical complexity for an exemplary, molecule-rich dark molecular cloud.

PRIOR SEARCHES

Previous searches have predominantly focused on nitrogen-bearing heterocycles, with the only exceptions being the O- and Si-bearing species oxirane,[25] propylene oxide,[26] furan,[27−29] and silicon di- and tricarbides.[30,31] To the best of our knowledge, there have not been any searches for sulfur-bearing heterocycles. The emphasis on N-heterocycles is likely motivated by their significance in biological molecules, combined with the availability of spectroscopic data. Below we outline the prior searches for nitrogen- and oxygen-bearing

heterocycles that have been conducted. For completeness, we note that two silicon-bearing heterocycles have been detected toward IRC+10216, silicon dicarbide (silacyclopropynylidene, SiC_2),[30] and silicon tricarbide (SiC_3).[31]

Detections. *Oxirane, c-C_2H_4O.* Oxirane (ethylene oxide) is the simplest oxygen-bearing heterocycle. It was first detected by Dickens et al. using lines from the Nobeyama 45-m, Haystack 140-ft, and SEST 15-m telescope observed toward Sagittarius B2 (Sgr B2).[25] It has since been detected in various interstellar environments including low mass protostars[32] and prestellar cores.[33]

2-Methyloxirane, c-$CH_3C_2H_2O$. The functionalized heterocycle, 2-methyloxirane (propylene oxide) was detected by McGuire et al. in GBT 100-m and Parkes 64-m observations of Sgr B2.[26]

Tentative Detections. *2H-Azirine, C_2H_3N.* 2H-Azirine, c-C_2H_3N, and its reduced form aziridine (ethylenimine), c-C_2H_5N, are the simplest N-heterocyclic compounds. 2H-Azirine has been previously searched for in Sgr B2(N-LMH) and Orion KL, and a tentative detection was reported.[34−36]

Aziridine, C_2H_5N. Two groups have reported tentative detections of aziridine. Dickens et al.[28] reported two detected lines toward hot cores G327.3, G10.47, and possible weak emissions toward G34.3, Sgr B2(N), and NGC6334. Kuan et al. also reported a tentative detection of aziridine toward hot cores Orion KL and W51 e1/e2.[34,35]

Nondetections. *Pyrrole, C_4H_4NH.* Pyrrole, or more specifically 1H-pyrrole, is a five-membered ring analogous to cyclopentadiene, in which a carbon is substituted for a nitrogen atom. Two other tautomers of pyrrole exit: 2H-pyrrole, which has the double bonds at positions 1 and 3, and 3H-pyrrole, which has the double bonds at positions 1 and 4. Pyrrole has been searched for toward the hot core Sgr B2(N)[27,37] as well as the cold molecular cloud TMC-1.[27] Toward TMC-1, Kutner et al.[27] derived an upper limit of 4×10^{12} cm^{-2}.

Imidazole, $C_3N_2H_4$. Imidazole is a diazole (five-membered aromatic heterocycle with two nitrogen atoms) of particular biological relevance. This ring system is present in important biological building blocks, such as histidine and the related hormone histamine. In addition, many pharmaceutical drugs
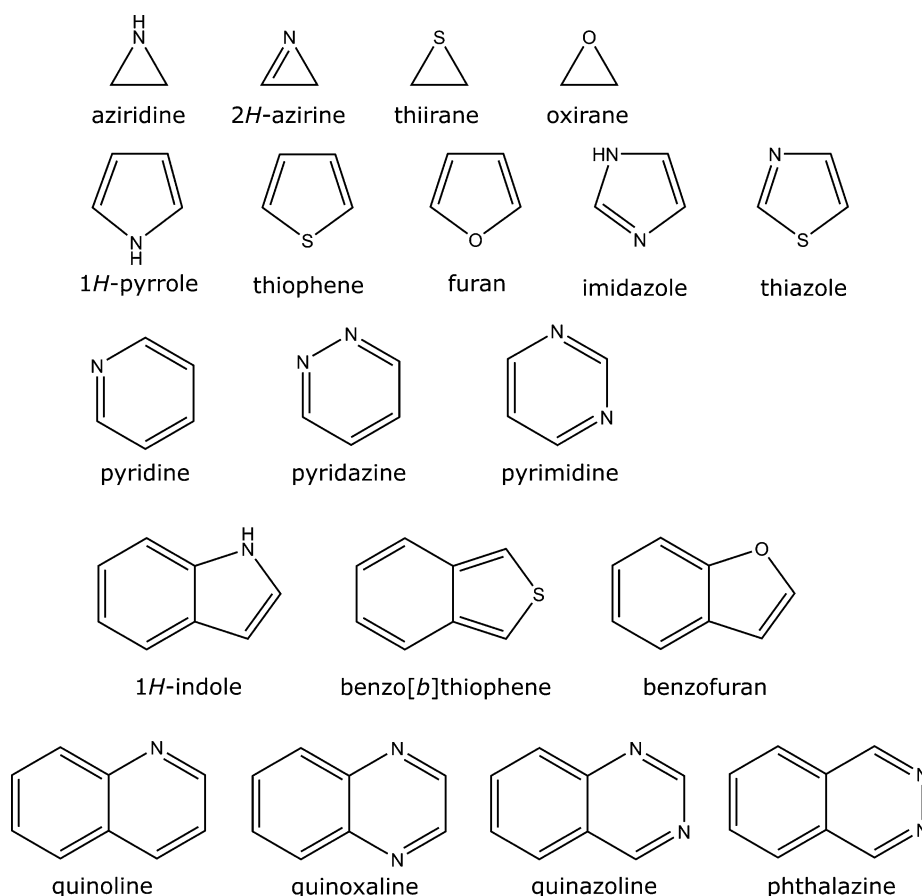
Figure 2. Chemical structures of the heterocycles included in our analysis.

contain an imidazole ring.[38] When fused to a pyrimidine ring, it forms a purine, which is the most widely occurring nitrogen-containing heterocycle in nature.[39] Despite its relevance on earth, imidazole has only been searched for toward Sgr A and Sgr B2(N).[40,41] Giuliano et al.[41] recently searched for imidazole in Sgr B2(N), following their improved laboratory spectroscopy, and reported a nondetection.

Pyridine, C_5H_5N. Pyridine is a six-membered heterocycle, structurally related to benzene, with one CH replaced by a nitrogen atom. The pyridine ring occurs in many important compounds, including agrochemicals, pharmaceuticals, and vitamins.[42] Pyridine has been searched for toward hot cores Sgr B2,[43,44] Sgr A,[44] Orion A,[44] and the circumstellar envelopes of carbon-rich stars, IRC+10216 and CRL 618.[45]

Pyrimidine, $C_4H_4N_2$. Pyrimidine is an aromatic heterocycle similar to pyridine. One of the three diazines (six-membered aromatic heterocycles with two nitrogen atoms) has the nitrogen atoms at positions 1 and 3 in the ring. The other diazines are pyrazine (nitrogen atoms at the 1 and 4 positions) and pyridazine (nitrogen atoms at the 1 and 2 positions), which have not been previously searched for in the ISM. Pyrimidine occurs widely in nature, including in the nucleotides cytosine, thymine and uracil, and thiamine (vitamin B1) and alloxan, as well as in many synthetic drugs.[46] Pyrimidine was first searched for in 1973 by Simon and Simon toward the hot core Sgr B2(N).[43] Following the nondetection in Sgr B2(N), Irvine et al.[47] searched for pyrimidine in a handful of sources: TMC-1, L134N, W3 C, W3 (OH), Orion A, DR 21 (OH), S140, and IRC+10216. They reported an upper limit of 6×10^{12} cm^{-2} toward TMC-1. Kuan

et al.[34] later conducted a search for pyrimidine toward Sgr B2(N), Orion KL and W51 e1/e1.

Quinoline, C_9H_7N. Quinoline is one of the simplest polycyclic aromatic nitrogen heterocycles (PANHs), with a similar structure to naphthalene's but with one CH substituted for a nitrogen. Quinoline was searched for by Charnley et al.[45] toward the circumstellar envelopes IRC+10216, CRL 618, and CRL 2688.

Isoquinoline, i-C_9H_7N. Isoquinoline is a structural isomer of quinoline, with CH substituted for a nitrogen atom at the 2 position in the ring. Isoquinoline was likewise searched for by Charnley et al. toward the circumstellar envelopes IRC+10216, CRL 618 and CRL 2688.[45]

Furan, C_4H_4O. Furan is a five-membered aromatic heterocycle with four carbon atoms and one oxygen. It was first searched for by Kutner et al.[27] toward hot cores Sgr B2(N) and Orion A. Dickens et al.[28] searched for furan toward a number of sources: TMC-1(CP), Orion KL, Orion 3'N, G327.3-0.6, L134N(C), IRS 16293, NGC 6334F, Sgr B2(N), and W33A. Toward TMC-1(CP) they reported an upper limit of $(1-2) \times 10^{13}$ cm^{-2}. Most recently, Barnum et al.[29] reported an upper limit of 1×10^{12} cm^{-2} using the GOTHAM line survey.

■ OBSERVATIONS

We performed a search toward TMC-1 using the third data reduction of the GOTHAM collaboration survey, hereafter referred to as DR3. Details of the source, observations, and data reduction methods can be found in McGuire et al.[4,48] Here, we provide a brief summary. Observations were performed with the 100-m Robert C. Byrd Green Bank

Telescope with the project codes GBT17A-164, GBT17A-434, GBT18A-333, and data from project GBT19B-047.

The first and second data release of GOTHAM (hereafter referred as DR1 and DR2) comprise observations obtained between February 2018 and May 2019 (DR1) and until June 2020 (DR2).[4,48] The GOTHAM observations used here are DR3, which comprises observations made through April 2021. DR3 extends the frequency coverage to 7.906–35.434 GHz with a few gaps and improved the sensitivity in some frequency coverage already covered by DR2.

The pointing was centered on TMC-1 CP at (J2000) α = 04^{h}41^{m}42.50^s δ = +25°41′26.8″. The spectra were obtained through position-switching to an emission-free position 1° away. Pointing and focusing was refined every 1–2 h on the calibrator J0530+1331. Flux calibration was performed with an internal noise diode and Very Large Array (VLA) observations (Project TCAL0003) of the same calibrator used for pointing, resulting in a flux uncertainty of ~20%.[48]

Our search includes 19 heterocycles whose chemical structures are shown in Figure 2. The molecules chosen include small, single-ring heterocycles, as well as two-ring species and those with two heteroatoms in the ring. Factors influencing our choice of molecules included chemical complexity (i.e., starting with small, single-heteroatom species), prior searches, the availability of spectroscopic data, and the recommendations produced by the unsupervised machine learning model of Lee et al.[49] Our search is heavily biased toward nitrogen heterocycles, which is perhaps not surprising given the prevalence of nitrogen-containing molecules already detected in TMC-1, their dominance in previous searches, and their biological relevance.

Figure 1 shows a visualization of the chemical space we have chosen to prioritize for this work: many heterocycles were not explored, including some unsubstituted heterocycles for which sufficient spectroscopic data could not be sourced. This list includes the four-membered rings azete, 2H-oxete, and 2H-thiete (and their saturated counterparts azetidine, oxetane, and thietane) and six-membered rings containing sulfur or oxygen (pyrans and thiopyrans) as well as oxygen and sulfur containing polycyclic heterocyles (chromene, thiochromene). Polycyclic heterocycles containing more than one heteroatom were likewise not considered in this study. Structural isomers and/or tautomers may also be considered in future studies, for example, 2H-pyrrole, isobenzofuran, isoindole, and isoquinoline.

RESULTS AND DISCUSSION

Upper Limits Analysis. In the third data release from the GOTHAM collaboration, we could not identify individual lines belonging to the heterocycles in Table 1. Without individual line detections, we applied Bayesian forward modeling with Markov chain Monte Carlo (MCMC) sampling to establish upper limits to the column density of these molecules in TMC-1. These methods have been described in detail previously[71] and have been used in combination with spectral line stacking to positively identify new species in TMC-1 without individual observable transitions.

These methods are implemented in molsim,[72] wrapping the affine-invariant sampler emcee[73] and uses ArviZ[74] for analysis and visualization. Here, we encode knowledge about the physical conditions of TMC-1 and the heterocyclic species through the choice of prior distributions. For all species, we

Table 1. Upper Limit Column Densities for All Investigated Heterocycles Determined as the 97.5th Percentile of the Highest Posterior Density Credible Interval Summed over All Four Components of TMC-1[a]

species	formula	column density upper limit ($\log_{10}$ cm^{-2})	dipole moment (D)	no. of lines	refs
aziridine	C_2H_5N	13.29	1.36	155	50
2H-azirine	C_2H_3N	12.10	2.07	34	51
thiirane	C_2H_4S	12.33	1.84	46	52
oxirane	C_2H_4O	12.26	1.88	6	53, 54
1H-pyrrole	C_4H_5N	12.00	1.74	382	55, 56
thiophene	C_4H_4S	13.10	0.55	68	57
furan	C_4H_4O	12.93	0.66	103	29
imidazole	$C_3H_4N_2$	12.09	3.60	1456	41
thiazole	C_3H_3NS	12.85	1.29	372	58, 59
pyridine	C_5H_5N	11.88	2.22	775	60
pyridazine	$C_4H_4N_2$	12.33	4.22	1503	61, 62
pyrimidine	$C_4H_4N_2$	12.62	2.33	659	63−65
1H-indole	C_8H_7N	11.60	1.59	4203	66
benzo[b]thiophene	C_8H_6S	13.11	0.64	1562	67
1-benzofuran	C_8H_6O	12.01	0.72	1147	68
quinoline	C_9H_7N	12.38	2.01	9022	69
quinoxaline	$C_8H_6N_2$	13.06	0.59	1128	70
quinazoline	$C_8H_6N_2$	10.61	2.89	10487	70
phthalazine	$C_8H_6N_2$	10.94	5.45	5189	70

[a]The upper limits are reported as log column densities in units of cm^{-2}. The table also reports the largest dipole moment component in the principal axis system of each molecule in units of Debye and the total number of lines included in the analysis.

used Gaussian priors consistent with the posterior distributions derived from our earlier analysis of benzonitrile,[48] which includes four velocity components with individual source sizes and radial velocities, as well as a shared excitation temperature and line width parameter. The excitation temperature prior was adjusted upward from that earlier analysis to a mean value of T_{ex} = 8.0 K, in better agreement with more recent analyses in TMC-1 by both the GOTHAM and QUIJOTE projects.[75−77] Uniform priors spanning 16 orders of magnitude for the four column densities were used to minimize the influence of the prior choice on the derived column density upper limits. In all cases, sampling of 200 Markov chains with 10 000 steps led to acceptable convergence ($\hat{r} \lesssim 1.1$) of all parameters. In Table 1, we report the 2σ upper limit log column densities for all species, corresponding to the 97.5th percentile of the highest density credible interval of the resultant posterior distributions. A representative corner plot of the column density posterior distributions for the species 1H-pyrrole appears in Figure 3. The diagonal traces correspond with the marginalized likelihood for each column density, while the off-diagonal contour plots show the covariance between each parameter. The upper limit is indicated by the break in the marginalized 1-D distributions, and its value appears above each plot. The long-tailed distributions toward zero column densities are characteristic of posterior distributions representing upper limits.

For those species previously searched for in TMC-1 (1H-pyrrole, pyrimidine, furan),[27,28,47] we find that our data provide a more stringent upper limit. In the case of furan, which was previously searched for in TMC-1 by some of us, the upper
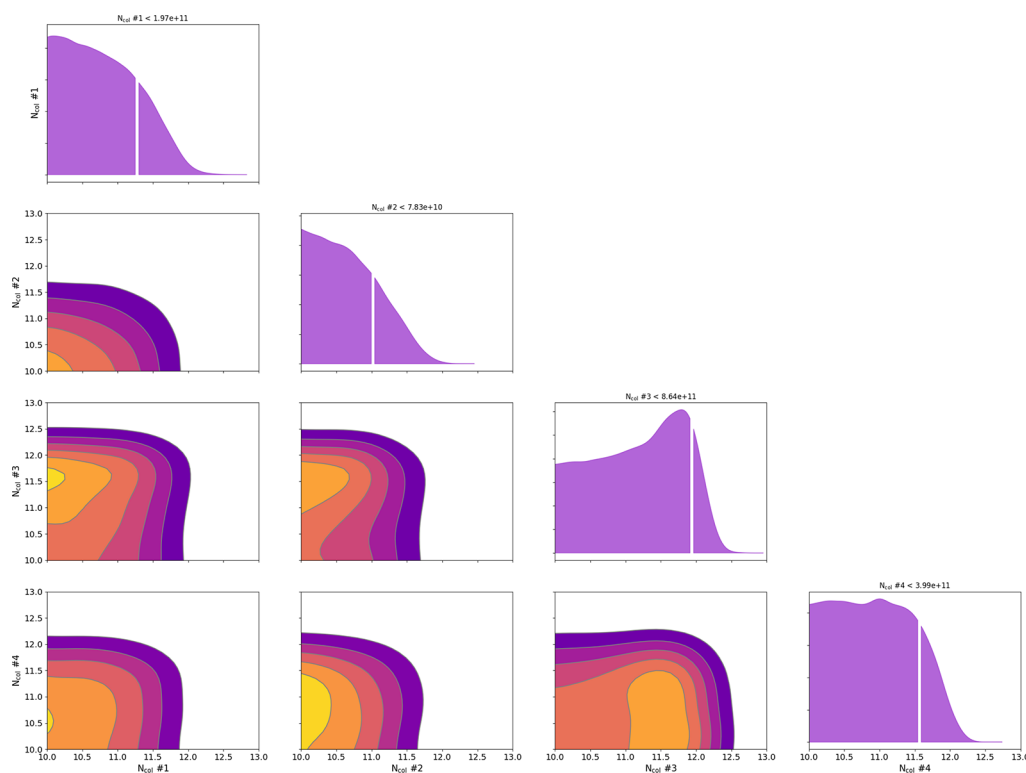
Figure 3. Corner plot of the marginal posterior distribution of the four column densities for 1*H*-pyrrole. Tick marks on all axes represent orders of magnitude of the column density in units of cm^{-2}. In all four velocity components, a long-tailed distribution toward low column densities indicates a nondetection of this species in the data. The derived upper limit is indicated by the gap in the marginalized 1-D distribution for each component, and the upper limit value appears above.

limit presented here represents a more conservative determination. The difference between our previous and current values is attributed to a difference in assumptions between the two analyses. Here, we allow the source size to vary and use uniform column density priors, rather than fixing the source sizes and using Gaussian column density priors.

To facilitate comparison with other upper limit determinations in the literature, we also derived upper limits for four heterocycles using a more traditional, frequentist single-line analysis. For each molecule, we used `molsim` to simulate a spectrum at the column density and excitation conditions of benzonitrile (T_{ex} = 8 K) using a single velocity component with a width of 0.5 km/s at v_{lsr} = 5.85 km/s.[78] We then identified the brightest line covered by our spectra, prioritizing transitions that lie in regions where the root-mean-square (RMS) noise is low and applied the formalism of Hollis et al.[79] to determine the upper limit column density.

Here, T_{ex} is the assumed 8 K excitation temperature (K); T_{bg} is the background continuum temperature and assumed to be 2.7 K; k is Boltzmann's constant ($J K^{-1}$); h is Planck's constant (J s); Q is the rotational partition function at T_{ex}; E_u is the upper state energy of the transition (K); $\int T \, dV$ is the upper limit velocity-integrated line area (K·km/s), which is taken as the product of the 2σ rms noise level and the assumed 0.5 km/s line width; $S_{ij}\mu^2$ is the transition line strength ($Debye^2$); and B and η_B are the beam filling factor and beam efficiency, which are both assumed to be 1.0 for this analysis.

$$N_T = \frac{1}{2} \frac{3k}{8\pi^3} \sqrt{\frac{\pi}{\ln 2}} \frac{Q \, e^{E_u/T_{ex}} \int T \, dV}{B \nu S_{ij}\mu^2 \eta_B} \frac{1}{1 - \frac{e^{h\nu/kT_{ex}}-1}{e^{h\nu/kT_{bg}}-1}}$$

(1)

For furan, the brightest expected line is the $J_{K_a,K_c} = 2_{1,2} \rightarrow 1_{1,1}$ transition at 23 259.2 MHz (see Figure 4). Using the sensitivity
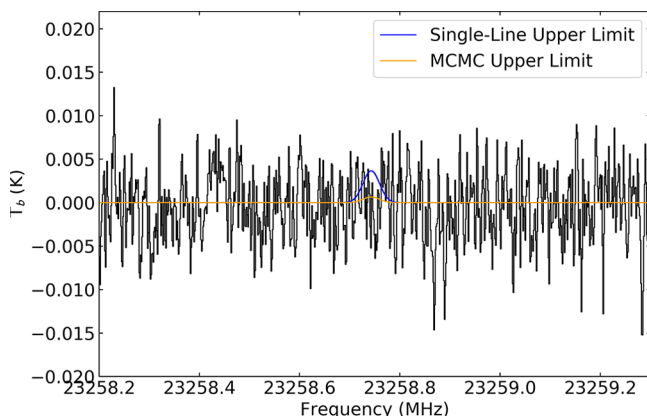
Figure 4. GOTHAM DR3 spectrum (black trace) at the brightest line expected for furan ($J_{K_a,K_c} = 2_{1,2} \rightarrow 1_{1,1}$). Simulations plotted in blue and orange correspond to the upper limit column densities derived using the single-line and Bayesian stacking analyses employed in this work. Both simulations were made with T_{ex} = 8 K and v_{lsr} = 5.85 km/s.

of our survey at this frequency, we calculate an upper limit log column density of 13.68 cm^{-2} for furan based on this line. The order of magnitude difference between this approach and the MCMC analysis can be attributed to our consideration of the full spectrum. For furan, 103 individual lines were used in the MCMC analysis, after removing any lines from the analysis that appear near interloping lines of another species within a

± 0.5 km/s window in velocity space. Under the assumptions that all transitions are similarly bright and that we only have white noise present in our data, we would expect the RMS of a stacked spectrum containing all of these lines (and thereby, the derived upper limit column density) to go approximately as $1/\sqrt{n}$ where n is the number of stacked lines. The single line analysis of furan is representative of this behavior.

When we apply this method to imidazole, we find that a bright blend of three hyperfine components of the $J_{K_aK_c} = 3_{1,3} \rightarrow 2_{1,2}$ transition is expected at 33 397.38 MHz. Using this single feature, we derive an upper limit log column density of 12.86 cm^{-2} for imidazole, which is almost 1 order of magnitude larger than the upper limit we place using the MCMC approach. In contrast to furan, however, a total of 1456 lines were used in the MCMC analysis, so this does not follow the $1/\sqrt{n}$ scaling law discussed above. This is likely due to the inclusion of hyperfine structure in our catalog for this molecule, which often produces blended lines that contribute the same information despite being counted as individual lines. For quinazoline, we calculate a log upper limit of 12.50 cm^{-2} based on nine blended lines of the $J_{K_aK_c} = 14_{0,14} \rightarrow 13_{0,13}$ at 26 536.73 MHz. This is almost 2 orders of magnitude larger than what we obtain from a Bayesian analysis of all 10 487 covered transitions, meaning a large fraction of those transitions contribute unique information to the MCMC analysis. Finally, for 1H-pyrrole, we analyzed the $J_{K_aK_c}$ (F) = $3_{0,3}(4) \rightarrow 2_{0,2}(3)$ line at 31 727.38 MHz to obtain a log upper limit column density of 13.43 cm^{-2}.

As expected, we found that all upper limits derived using a frequentist single-line analysis were larger than those from the MCMC results. The degree by which these upper limits varies is largely determined by the number of lines included in the analysis, the fraction of lines that are not blended, and the fraction that are expected to have significant emission at an excitation temperature of 8 K.

To describe the relationship between physical properties of molecules and their derived upper limit, Figure 5 plots the column density upper limits as a function of the largest dipole moment component in the principal axis system of each molecule. The fitted model shows that with few exceptions, the
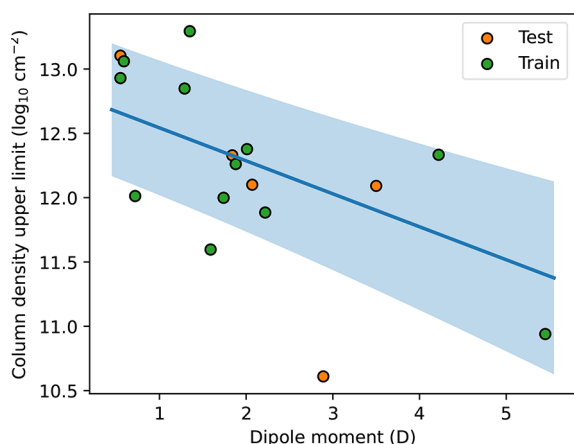
upper limit determinations for heterocycles are a function of their physical properties: barring abnormal chemical dynamics (e.g., preferred reactions), one can predict the expected upper limit of other heterocycles bounded by a credible interval, simply from the dipole moment.

We can compare the upper limits of the heterocycles to the derived column densities for the carbocyclic molecules that have been detected in TMC-1 thus far. Pyridine is found to be depleted compared to benzonitrile,[5] its closest detected carbocyclic counterpart (log column density of 11.88 versus 12.24 cm^{-2}), suggesting that pyridine is at most half as abundant as benzonitrile. We would therefore expect the CN-substituted pyridine isomers to be substantially lower in abundance than benzonitrile. In the case of the five-membered rings, cyclopentadiene has been detected recently by Cernicharo et al.[7] who derived a log column density of 13.08 cm^{-2}. This suggests that 1H-pyrrole, thiophene, and furan are at least 12, 9.5, and 1.4 times less abundant than their carbocyclic counterpart, further confirming the depletion of heterocycles in TMC-1. Another interesting comparison is between the N-, S-, and O-substituted counterparts of indene: indole, benzo[b]thiophene, and 1-benzofuran. Indole and benzofuran are at least $\sim$20 times and 10 times less abundant than indene, respectively, while the upper limit for benzo[b] thiophene is similar to the detected abundance of indene.[5] As discussed above, molecules with low dipole moments generally have less well constrained upper limits, partially explaining the higher upper limit of benzo[b]thiophene. Our results suggest a significant depletion of heterocycles relative to pure carbocycles in TMC-1.

It is noteworthy that for several of the species considered, we observe a distinct peakedness to the column density posterior distributions for one or more velocity components. Manual inspection of the spectral windows used in the MCMC analysis confirms the absence of interloper lines from other detectable species, which could be responsible for these peaked distributions. Instead, we hypothesize that correlated (i.e., "red") noise in the frequency spectrum is the origin of these unexpected posterior distributions. In the calculation of the log likelihood function, our current MCMC implementation assumes only white noise in the data set, namely, that the measurement uncertainty of any single channel in the frequency spectrum is uncorrelated with noise in a neighboring channel. While this assumption captures most of the noise in the astronomical data, it is a first approximation to the noise only. As a result of aperiodic fluctuations in the source brightness over the course of the observational time, red $\left(\frac{1}{f^2}\right)$

Figure 5. Relationship between molecular properties (dipole moment) and the derived upper limit. The blue line and shaded band correspond to the mean and $\pm 1\sigma$ uncertainty of a Bayesian ridge regression model. Scatter points are color coded on the basis of their training/test split.

noise also contributes to the noise floor. Beyond intrinsic sources of noise, polynomial baseline fitting in the data reduction step has the potential to introduce additional correlations between channels in the frequency spectrum. Neglecting these correlations in the noise can introduce bias into our inferences, especially as the signals of interest approach and go below the noise floor. For this reason, we do not interpret any peaks in the column density posterior distributions as meaningful and instead interpret all column densities as upper limits only. In a future implementation, we plan to increase the sophistication of our MCMC analysis with noise modeling. By explicit consideration of the off-diagonal components of the covariance matrix used to calculate the likelihood function, we can account for correlated noise in the

data set and begin to peer below the noise floor of the GOTHAM data.

Discussion on the Formation and Stability of Heterocycles in Cold Molecular Clouds. The quantitative visualization of chemical space in Figure 1 underscores the structural similarities between the unobserved heterocycles and previously observed molecules in TMC-1. While the heterocycles do overlap with newly observed aromatic carbocycles, they cluster toward the boundaries of known chemical space in TMC-1. Despite their structural similarity, our null detections for a wide range of heterocycles point to a unique chemistry of these species relative to the pure carbocyclic species, which suggests chemically defined bounds on the complexity of molecules found in TMC-1. Given that these heterocycles are highly stable terrestrially, it is likely a matter of dynamics that dictates their absence, and lends importance to finding kinetically viable pathways to their formation.

The formation of heterocycles in TMC-1 would require either chemical pathways that can operate at temperatures below 10 K or their inheritance from high-temperature sources, such as circumstellar envelopes. While a number of aromatic molecules have now been detected in TMC-1, it remains unclear whether these molecules form in situ by bottom-up mechanisms from small precursors or by top-down mechanisms through the destruction of large PAHs or interstellar dust grains.[5] It is expected that PAHs composed of less than ~20−30 atoms do not survive transport from the diffuse ISM to cold molecular clouds due to their degradation by ultraviolet photons.[80] While work from the combustion chemistry community has shown that high-temperature routes can produce PAHs and nitrogen- and oxygen-substituted PAHs (PANHs and PAOHs), several low-temperature routes have also been proposed that may operate in TMC-1. Below, we summarize potential formation routes to heterocycles that could operate under the conditions of TMC-1.

Formation of the First Heterocyclic Rings. Single-ring heterocycles are expected to be building blocks for larger N-, O-, and S-substituted PAHs, thus understanding their formation is the first step in determining whether biological precursor heterocycles can exist at the early stages of star formation. Formation routes to the smallest heterocycles, aziridine, 2*H*-azirine, oxirane, and thiirane, have not been well explored. Crossed-beam experiments suggest the reaction of N(^{2}D) with ethylene (C_2H_4) can form 2*H*-azirine; however, isomerization to the more stable isomer acetonitrile (CH_3CN) is expected, even under collision-free conditions.[81] Recent work has shown the formation of 2*H*-azirine in interstellar ice analogues of acetylene and ammonia after irradiation with energetic electrons.[82] The suggested mechanism involves the reaction of imidogen ($NH(a^1\Delta)$) with acetylene through addition to the carbon−carbon triple bond leading to 1*H*-azirine, which may isomerize via a hydrogen shift to 2*H*-azirine via a barrier of 108 kJ mol^{-1}.

Oxirane formation has been explored in more detail, motivated by its astronomical detection in the ISM.[83] Similar to azirine, oxirane has been shown to form in electron[84] and photon[85] irradiated ices, this time containing carbon dioxide (a source of suprathermal O atoms) and ethylene. Oxirane has also been shown to form ethylene oxide during the coaccretion of thermalized atomic oxygen and ethylene onto a solid substrate. In the gas phase, oxirane has been proposed to form by the dissociative recombination of $C_2H_5O^+$ with electrons,[25] where $C_2H_5O^+$ is formed by

$$CH_3^+ + C_2H_5OH \rightarrow C_2H_5O^+ + CH_4 \tag{2}$$

$$H_3O^+ + C_2H_2 \rightarrow C_2H_5O^+ + h\nu \tag{3}$$
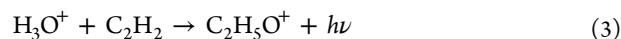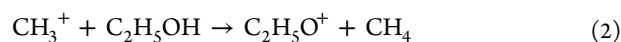
The importance of this reaction has been difficult to quantify due to the lack of detections of ethanol, H_3O^+, C_2H_2, and CH_3^+ in cold cores, combined with uncertainties in the experimental branching ratios. Another plausible gas-phase source of oxirane at low temperature is the reaction between O atoms and the ethyl radical (C_2H_5), but the branching ratio compared to those of its more stable isomers, acetaldehyde and vinyl alcohol, is unknown.

A reaction mechanism to form thiirane, $S(^1D) + C_2H_4$, has been inferred by Balucani due to its similarity to $N(^1D)$ reactions.[86] The electrophilic $S(^1D)$ atom adds, without a barrier, to the double bond of ethylene, forming the internally excited cyclic intermediate thiirane. Various ring-opening and isomerization pathways exist to convert thiirane into more stable products, and thus it is unclear if this reaction can produce thiirane under dense cloud conditions. Lastly, while this reaction has been found to be rapid down to 23 K, thiirane was not identified experimentally.[87]

Limited experimental and theoretical data exist for the formation of the five-membered oxygen, nitrogen, and sulfur heterocycles. Furan has been shown to form in the reaction between CH and acrolein at room temperature.[88] The major products were found to be 1,3-butadienal (60 ± 12)% and furan (17 ± 10)%. Reactions of OH and NH with 1,3-butadiene have been proposed to form furan and pyrrole but more data are needed on the reaction rate constants and products at low temperature.[3,89]

The formation of the six-membered nitrogen heterocycle, pyridine, in the interstellar medium has been an active area of research. Chemical models of Titan's atmosphere have proposed that pyridine may form by radical-mediated reactions of hydrogen cyanide (HCN) with acetylene (C_2H_2);[90] however, this mechanism has not been experimentally verified and may not operate under dense cloud conditions. A similar mechanism involving sequential reactions of HCN with the acetylene radical cation has been shown experimentally to produce the pyrimidine ion.[91] In addition, recent ab initio molecular dynamics simulations and density functional theory computations have shown that pyridine ions can form during the ionization of van der Waals clusters of HCN and C_2H_2.[92]

Formation of pyridine through ring expansion of pyrrole by methylidyne (CH) has been observed in the gas phase by Soorkia et al. (2010):[93]

$$CH + C_4H_5N \rightarrow c\text{-}C_5H_5N + H \tag{4}$$
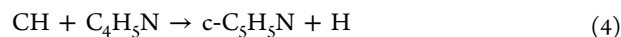
However, since pyrrole has likewise not been detected in the ISM, the formation of interstellar pyridine from pyrrole cannot be observationally constrained. Another neutral−neutral route to pyridine, the reaction of CN with 1,3-butadiene, has been explored in a combined experimental and theoretical study.[94] The formation of the aliphatic product cyano-1,3-butadiene, however, was shown to be the major product.

$$CN + C_4H_6 \rightarrow c\text{-}C_5H_5N + H \tag{5}$$

$$CN + C_4H_6 \rightarrow CN\text{-}C_4H_5 + H \tag{6}$$
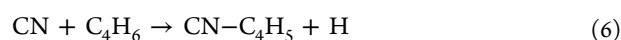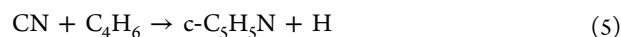
The reaction of the cyano vinyl radical with vinyl cyanide is a promising route to pyridine at low temperature and has been verified experimentally, albeit at high temperatures in a pyrolytic reactor.[95]

$$C_2H_3CN + C_2H_2CN \rightarrow C_5H_5N + CN \tag{7}$$
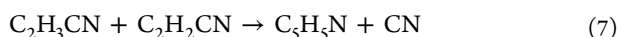
Supporting electronic structure calculations indicate that this reaction is exoergic and proceeds without an entrance barrier; therefore, it is likely to operate at low temperature. Future explorations of this reaction under low-temperature thermal conditions are desirable, especially to determine the branching ratio of pyridine and other potential products such as 1,4-dicyano-1,3-butadiene.

Fondren et al.[96] studied the reaction of pyridine and pyrimidine with a series of ions in a selected ion flow tube. They inferred from these experiments that efficient ion–molecule radiative association reactions with HCN could form pyridine (and pyrimidine) from smaller ions:

$$C_4H_4^+ + HCN \rightarrow c\text{-}C_5H_5N^+ + h\nu \tag{8}$$

$$C_3H_3N^+ + HCN \rightarrow c\text{-}C_4H_4N_2^+ + h\nu \tag{9}$$
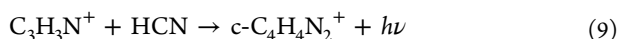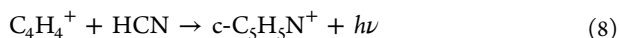
However, such radiative association reactions are challenging to measure in the laboratory, and it remains unclear if the reactions above are efficient at low temperature. Balucani et al.[97] investigated a pathway to pyridine via $N(^2D)$ reaction with C_6H_6, leading to a chain of unstable intermediate products that may decay to c-C_5H_5N. However, more recent computational work indicates that this reaction produces pyrrole, rather than pyridine, and that the major product channel is hydrogen cyanide plus a cyclopentadienyl radical ($\sim$90%).[98]

Krasnopolsky[99] suggested another a neutral–neutral pathway to form pyridine; however, it is considered more likely that this reaction forms the aliphatic isomer $C_2H_5C_3N$:[100]

$$C_3N + C_2H_6 \rightarrow c\text{-}C_5H_5N + H \tag{10}$$
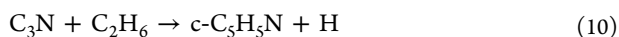
N- and O-heterocyclic molecules have been identified in the room-temperature residues resulting from the ultraviolet irradiation of the carbocyclic aromatic molecules benzene or naphthalene mixed in ices containing H_2O and NH_3.[101] Nitrogen heterocycles identified include some of those searched for in our data: pyridine and quinoline. The oxygen-bearing heterocycles detected include the lactones phthalide ($C_8H_6O_2$), coumarin ($C_9H_6O_2$), and isocoumarin ($C_9H_6O_2$); however, it was noted that small O-heterocycles like furan could not be detected with their technique.

Formation of Heterocyclic PAHs and Nucleobases. Like pure hydrocarbon PAHs, heterocyclic PAHs have been thought traditionally to form in high-temperature environments through barriered reactions. One route suggested to operate in circumstellar envelopes is the reaction between the meta-pyridyl radical with two acetylene molecules via a hydrogen abstraction/acetylene addition (HACA) type reaction mechanism.[102] Following the formation of single-ring heterocyles, it has been suggested that formation of subsequent rings resulting in PANHs, PAOHs, and PASHs should be efficient in the cold ISM. Pyridine has been suggested to be an important building block in the formation of more complex PANHs. Pyridine can be photolyzed to form pyridyl radicals (C_5H_4N),[103] which have been shown to react without an entrance barrier with 1,3-butadiene to form the PANHs 1,4-dihydroquinoline, and quinoline (as well as the iso-isomers), respectively.[102,104]

Ricca et al.[90] proposed a route involving radical-mediated addition reactions of HCN and acetylene to form a pure aromatic ring. If hydrogen cyanide is abundant, the acetylene polymerization chemistry that leads to PAH formation in the circumstellar envelopes of AGB/post-AGB carbon stars can lead to the incorporation of nitrogen into the PAH backbone. They show that inclusion of a nitrogen atom into a PAH could promote the formation of additional hydrocarbon rings by lowering the ring closing barrier. Ultimately, these molecules could contribute to the formation of much larger PANHs that are believed to play an important role in interstellar chemistry.

The astrochemical link between simple, unsubstituted heterocycles and the more complex purine and pyrimidine nucleobases has not yet been made. Oba et al.[105] have detected all three pyrimidine (cytosine, uracil, and thymine) and three purine nucleobases (adenine, xanthine, and hypoxanthine) in the organic residue of interstellar ices composed of H_2O, CO, NH_3, and CH_3OH after exposure to UV photons. It is clear that heterocycles and even prebiotic nucleobases can form under conditions expected to be present in some regions of interstellar space, but the chemical mechanisms linking small molecules to the molecules of life remain unknown and will motivate future studies.

Destruction of Heterocycles and the Effect on Their Detectability. Peeters et al.[106] compared the photolytic stabilities of benzene and pyridine (as well as pyrimidine and s-triazine) in matrix isolation experiments. Their results indicate N-heterocycles photolyze rapidly and their stability decreases with the increasing number of N atoms in the ring. The authors calculated that these N-heterocycles in the gas phase would be destroyed in 10–100 years in the diffuse ISM, while in the Solar System 1 AU from the Sun they would not survive beyond several hours. They suggested that the only environment where small N-heterocycles could survive is in dense clouds that are shielded from intense UV radiation. Pyridine and pyrimidine, but not the triply N-substituted ring s-triazine, could survive the average lifetime of a dense cloud. Photolytic stability data do not exist for the doubly N-substituted PANHs that we searched for here, so it is unclear whether molecules like the $C_8H_6N_2$ isomers could survive. Extrapolating from their data on pyrimidine, we expect that imidazole and pyridazine could likely survive destruction by UV photons in dense clouds, but more data are required to confirm this. It has not yet been reported how long these molecules and other heterocycles can survive in ices. In addition, the radiolytic stability of heterocycles to cosmic rays should be quantitatively investigated.

Destruction of heterocycles through reactions are important to consider not only because they can potentially help explain their nondetection in TMC-1 but also because they can help determine molecules that may serve as detectable chemical proxies. Cyano-substituted aromatics have been shown to be good chemical proxies for small aromatics and PAHs due to the fact that CN radicals are likely to react without barriers with the double bonds of the aromatic ring.[107,108] Because heterocycles typically lack the symmetry present in unsubstituted aromatics, the multiple CN-substitution sites decrease the chances of detecting a specific isomer.

Recent theoretical work has suggested hydrogenated versions of heterocycles may serve as potential chemical proxies in dense clouds, due to the high H abundance, the ability of H to react via tunnelling, and the efficient diffusion of H on interstellar dust grains.[109] The authors show that many heterocycles react slowly with H and suggest that hydrogenated derivatives of furan (2,3-dihydrofuran, 2,5-dihydrofur-

an) and pyrrole (2,3-dihydropyrrole, 2,5-dihydropyrrole) are promising candidates for future interstellar searches.

Suggested Follow-Up Observations. Our comparison of the upper limits derived from the single line and the MCMC analyses suggests that consideration of all lines within the spectral window of our broadband survey considerably constrain the upper limit determination. This suggests that the detectability of particular molecules depends not only on intrinsic molecular properties like the dipole moment (Figure 5) but also on the spectral coverage and hence the total integrated line intensity for a molecule. Broadband line surveys thus serve an even more essential role in the search for new species in the ISM. Observations at higher frequencies would be beneficial, as the brightest lines for most molecules lie outside of our GOTHAM spectral coverage. For example, the brightest lines are expected to fall between 100−200 GHz for the three-membered rings and ∼50−70 GHz for the five- and six-membered rings.

In addition to broadband surveys as a tool to search for any heterocyclic species, targeted searches for chemically related molecules will serve an important role in constraining the chemistry of heterocycles in the ISM. As summarized in the preceding discussion, extensive experimental and theoretical studies have suggested plausible low-temperature heterocycle formation routes. While direct observation of the target heterocycles would provide the strongest support for proposed mechanisms, observations of the key reactive species en route to heterocycle formation can help to bolster or constrain these mechanisms. Some of these key molecules do not possess dipole moments (e.g., 1,3-butadiene), making their detection in TMC-1 challenging. Chemical proxies may be invoked, but only after careful validation through a combination of laboratory studies and kinetic models.

CN-substituted species have proven to be good choices as proxies, since the reaction between CN and unsaturated hydrocarbons is typically rapid,[110] and CN imparts a strong dipole moment on the resulting reaction product(s). The use of benzonitrile as a proxy for benzene has been confirmed through laboratory measurements of CN + C_6H_6 down to temperatures close to those in TMC-1.[108] C_2H-substituted aromatic heterocycles may likewise serve as good chemical proxies. Ethynyl has been shown to react rapidly with unsaturated hydrocarbons,[111,112] including benzene,[113] and C_2H-substituted cylic molecules, ethynyl cyclopentadiene and cyclopropenylidene, both of which have been recently detected toward TMC-1.[7,9]

Individual observations of key intermediate species in proposed chemical pathways will serve to motivate new experimental and theoretical studies and refocus observational efforts. Direct observations in other sources of aromatic and/or heterocyclic solid-phase vibrational modes with the James Webb Space Telescope (JWST) would be particularly useful in constraining the gas-ice partitioning of these molecules.

CONCLUSIONS

In this study, we have applied a Bayesian inference analysis to the third data reduction of the GOTHAM collaboration survey of TMC-1 to constrain the upper limit column densities for a large selection of one- and two-ring heterocycles. For those few species previously searched for in TMC-1, our new analysis improves the upper limit constraint on these species. We compare our upper limits derived from the MCMC analysis with those derived from a single line analysis and find that, for

all species, the consideration of all lines in the spectral window of the survey provides tighter constraints on the upper limit than consideration of only the single strongest line. In sum, our analysis confirms the peculiar depletion of heterocyclic species relative to the previously detected pure hydrocarbon cycles. Improvements to our MCMC analysis, as well as complementary observations of chemically related species, will help to further constrain the chemistry of heterocycles in the ISM.

■ ASSOCIATED CONTENT

ⓈI Supporting Information

The Supporting Information is available free of charge at https://pubs.acs.org/doi/10.1021/acs.jpca.2c01435.

Corner plots of column densities for all heterocycles investigated in this work (PDF)

■ AUTHOR INFORMATION

Corresponding Authors

Timothy J. Barnum − *Department of Chemistry, Union College, Schenectady, New York 12308, United States;* ⓐ orcid.org/0000-0002-9363-9844; Email: barnumt@union.edu

Brett A. McGuire − *Department of Chemistry, Massachusetts Institute of Technology, Cambridge, Massachusetts 02139, United States; National Radio Astronomy Observatory, Charlottesville, Virginia 22903, United States; Center for Astrophysics | Harvard & Smithsonian, Cambridge, Massachusetts 02138, United States;* ⓐ orcid.org/0000-0003-1254-4817; Email: brettmc@mit.edu

Ilsa R. Cooke − *Department of Chemistry, University of British Columbia, Vancouver, BC V6T 1Z1, Canada;* ⓐ orcid.org/0000-0002-0850-7426; Email: icooke@chem.ubc.ca

Authors

Mark A. Siebert − *Department of Astronomy, University of Virginia, Charlottesville, Virginia 22904, United States*

Kin Long Kelvin Lee − *Department of Chemistry, Massachusetts Institute of Technology, Cambridge, Massachusetts 02139, United States*

Ryan A. Loomis − *National Radio Astronomy Observatory, Charlottesville, Virginia 22903, United States*

P. Bryan Changala − *Center for Astrophysics | Harvard & Smithsonian, Cambridge, Massachusetts 02138, United States*

Steven B. Charnley − *Astrochemistry Laboratory and the Goddard Center for Astrobiology, NASA Goddard Space Flight Center, Greenbelt, Maryland 20771, United States*

Madelyn L. Sita − *Department of Chemistry, University of Virginia, Charlottesville, Virginia 22904, United States;* ⓐ orcid.org/0000-0002-7214-7058

Ci Xue − *Department of Chemistry, Massachusetts Institute of Technology, Cambridge, Massachusetts 02139, United States*

Anthony J. Remijan − *National Radio Astronomy Observatory, Charlottesville, Virginia 22903, United States*

Andrew M. Burkhardt − *Department of Physics, Wellesley College, Wellesley, Massachusetts 02481, United States*

Complete contact information is available at:
https://pubs.acs.org/10.1021/acs.jpca.2c01435

Notes

The authors declare no competing financial interest.

■ REFERENCES

(1) Tielens, A. G. G. M. *The Physics and Chemistry of the Interstellar Medium*; Cambridge University Press: Cambridge, MA, 2005.

(2) McGuire, B. A.; Burkhardt, A. M.; Kalenskii, S. V.; Shingledecker, C. N.; Remijan, A. J.; Herbst, E.; McCarthy, M. C. Detection of the aromatic molecule benzonitrile (c-C_6H_5CN) in the interstellar medium. *Science* **2018**, *359*, 202−205.

(3) McCarthy, M. C.; Lee, K. L. K.; Loomis, R. A.; Burkhardt, A. M.; Shingledecker, C. N.; Charnley, S. B.; Cordiner, M. A.; Herbst, E.; Kalenskii, S.; Willis, E. R.; et al. Interstellar detection of the highly polar five-membered ring cyanocyclopentadiene. *Nature Astronomy* **2021**, *5*, 176−180.

(4) McGuire, B. A.; Loomis, R. A.; Burkhardt, A. M.; Lee, K. L. K.; Shingledecker, C. N.; Charnley, S. B.; Cooke, I. R.; Cordiner, M. A.; Herbst, E.; Kalenskii, S.; et al. Detection of two interstellar polycyclic aromatic hydrocarbons via spectral matched filtering. *Science* **2021**, *371*, 1265−1269.

(5) Burkhardt, A. M.; Long Kelvin Lee, K.; Bryan Changala, P.; Shingledecker, C. N.; Cooke, I. R.; Loomis, R. A.; Wei, H.; Charnley, S. B.; Herbst, E.; McCarthy, M. C.; et al. Discovery of the Pure Polycyclic Aromatic Hydrocarbon Indene (c-C_9H_8) with GOTHAM Observations of TMC-1. *Astrophysical Journal Letters* **2021**, *913*, L18.

(6) Lee, K. L. K.; Changala, P. B.; Loomis, R. A.; Burkhardt, A. M.; Xue, C.; Cordiner, M. A.; Charnley, S. B.; McCarthy, M. C.; McGuire, B. A. Interstellar detection of 2-cyanocyclopentadiene, C_5H_5CN, a second five-membered ring toward TMC-1. *Astrophysical Journal Letters* **2021**, *910*, L2.

(7) Cernicharo, J.; Agúndez, M.; Cabezas, C.; Tercero, B.; Marcelino, N.; Pardo, J. R.; de Vicente, P. Pure hydrocarbon cycles in TMC-1: Discovery of ethynyl cyclopropenylidene, cyclopentadiene, and indene. *Astronomy & Astrophysics* **2021**, *649*, L15.

(8) Cernicharo, J.; Agúndez, M.; Kaiser, R. I.; Cabezas, C.; Tercero, B.; Marcelino, N.; Pardo, J. R.; de Vicente, P. Discovery of benzyne, o-C_6H_4, in TMC-1 with the QUIJOTE line survey. *Astronomy & Astrophysics* **2021**, *652*, L9.

(9) Cernicharo, J.; Agúndez, M.; Kaiser, R. I.; Cabezas, C.; Tercero, B.; Marcelino, N.; Pardo, J. R.; de Vicente, P. Discovery of two isomers of ethynyl cyclopentadiene in TMC-1: Abundances of CCH and CN derivatives of hydrocarbon cycles. *Astronomy & Astrophysics* **2021**, *655*, L1.

(10) Callahan, M. P.; Smith, K. E.; Cleaves, H. J.; Ruzicka, J.; Stern, J. C.; Glavin, D. P.; House, C. H.; Dworkin, J. P. Carbonaceous meteorites contain a wide range of extraterrestrial nucleobases. *Proc. Natl. Acad. Sci. U. S. A.* **2011**, *108*, 13995.

(11) Komiya, M.; Shimoyama, A.; Harada, K. Examination of organic compounds from insoluble organic matter isolated from some Antarctic carbonaceous chondrites by heating experiments. *Geochim. Cosmochim. Acta* **1993**, *57*, 907−914.

(12) Hayatsu, R. Orgueil Meteorite: Organic Nitrogen Contents. *Science* **1964**, *146*, 1291−1293.

(13) Folsome, C. E.; Lawless, J.; Romiez, M.; Ponnamperuma, C. Heterocyclic Compounds indigenous to the Murchison Meteorite. *Nature* **1971**, *232*, 108−109.

(14) Folsome, C. E.; Lawless, J. G.; Romiez, M.; Ponnamperuma, C. Heterocyclic compounds recovered from carbonaceous chondrites. *Geochim. Cosmochim. Acta* **1973**, *37*, 455−465.

(15) Hayatsu, R.; Studier, M. H.; Moore, L. P.; Anders, E. Purines and triazines in the Murchison meteorite. *Geochim. Cosmochim. Acta* **1975**, *39*, 471−488.

(16) van der Velden, W.; Schwartz, A. W. Search for purines and pyrimidines in the Murchison meteorite. *Geochim. Cosmochim. Acta* **1977**, *41*, 961−968.

(17) Stoks, P. G.; Schwartz, A. W. Uracil in carbonaceous meteorites. *Nature* **1979**, *282*, 709−710.

(18) Martins, Z.; Botta, O.; Fogel, M. L.; Sephton, M. A.; Glavin, D. P.; Watson, J. S.; Dworkin, J. P.; Schwartz, A. W.; Ehrenfreund, P. Extraterrestrial nucleobases in the Murchison meteorite. *Earth and Planetary Science Letters* **2008**, *270*, 130−136.

(19) Martins, Z. *Nitrogen Heterocycle Content of Meteorites and Their Significance for the Origin of Life* **2018**, *8*, 28.

(20) Burkhardt, A. M.; Loomis, R. A.; Shingledecker, C. N.; Lee, K. L. K.; Remijan, A. J.; McCarthy, M. C.; McGuire, B. A. Ubiquitous Aromatic Carbon Chemistry at the Earliest Stages of Star Formation. *Nature Astronomy* **2021**, *5*, 181−187.

(21) McGuire, B. A. 2021 Census of Interstellar, Circumstellar, Extragalactic, Protoplanetary Disk, and Exoplanetary Molecules. *Astrophysical Journal Supplement* **2022**, *259*, 30.

(22) Lee, K. L. K.; Patterson, J.; Burkhardt, A. M.; Vankayalapati, V.; McCarthy, M. C.; McGuire, B. A. Machine Learning of Interstellar Chemical Inventories. *Astrophysical Journal Letters* **2021**, *917*, L6.

(23) McInnes, L.; Healy, J.; Melville, J. UMAP: Uniform Manifold Approximation and Projection for Dimension Reduction. *arXiv:1802.03426v3* **2018**; https://arxiv.org/abs/1802.03426.

(24) Lee, K. L. K. Language models for astrochemistry (0.1.2). *Zenodo* 2021, DOI: 10.5281/zenodo.6299773.

(25) Dickens, J. E.; Irvine, W. M.; Ohishi, M.; Ikeda, M.; Ishikawa, S.; Nummelin, A.; Hjalmarson, A. Detection of Interstellar Ethylene Oxide (c-C_2H_4O). *Astrophysical Journal* **1997**, *489*, 753−757.

(26) McGuire, B. A.; Carroll, P. B.; Loomis, R. A.; Finneran, I. A.; Jewell, P. R.; Remijan, A. J.; Blake, G. A. Discovery of the interstellar chiral molecule propylene oxide (CH_3CHCH_2O). *Science* **2016**, *352*, 1449−1452.

(27) Kutner, M. L.; Machnik, D. E.; Tucker, K. D.; Dickman, R. L. Search for interstellar pyrrole and furan. *Astrophysical Journal* **1980**, *242*, 541−544.

(28) Dickens, J. E.; Irvine, W. M.; Nummelin, A.; Møllendal, H.; Saito, S.; Thorwirth, S.; Hjalmarson, A.; Ohishi, M. Searches for new interstellar molecules, including a tentative detection of aziridine and a possible detection of propenal. *Spectrochimica Acta Part A: Molecular and Biomolecular Spectroscopy* **2001**, *57*, 643−660.

(29) Barnum, T. J.; Lee, K. L. K.; McGuire, B. A. Chirped-Pulse Fourier Transform Millimeter-Wave Spectroscopy of Furan, Isotopologues, and Vibrational Excited States. *ACS Earth and Space Chemistry* **2021**, *5*, 2986−2994.

(30) Thaddeus, P.; Cummins, S. E.; Linke, R. A. Identification of the SiCC radical toward IRC + 10216: the first molecular ring in an astronomical source. *Astrophysical Journal* **1984**, *283*, L45−L48.

(31) Apponi, A. J.; McCarthy, M. C.; Gottlieb, C. A.; Thaddeus, P. Astronomical Detection of Rhomboidal SiC_3. *Astrophysical Journal* **1999**, *516*, L103−L106.

(32) Lykke, J. M.; Coutens, A.; Jørgensen, J. K.; van der Wiel, M. H. D.; Garrod, R. T.; Müller, H. S. P.; Bjerkeli, P.; Bourke, T. L.; Calcutt, H.; Drozdovskaya, M. N. The ALMA-PILS survey: First detections of ethylene oxide, acetone and propanal toward the low-mass protostar IRAS 16293−2422. *Astronomy & Astrophysics* **2017**, *597*, A53.

(33) Bacmann, A.; Faure, A.; Berteaud, J. Cold and Yet Complex: Detection of Ethylene Oxide in a Prestellar Core. *ACS Earth Space Chem.* **2019**, *3*, 1000−1013.

(34) Kuan, Y.-J.; Yan, C.-H.; Charnley, S. B.; Kisiel, Z.; Ehrenfreund, P.; Huang, H.-C. A search for interstellar pyrimidine. *Mon. Not. R. Astron. Soc.* **2003**, *345*, 650−656.

(35) Kuan, Y.-J.; Charnley, S. B.; Huang, H.-C.; Kisiel, Z.; Ehrenfreund, P.; Tseng, W.-L.; Yan, C.-H. Searches for interstellar molecules of potential prebiotic importance. *Adv. Space Res.* **2004**, *33*, 31−39.

(36) Charnley, S. B.; Ehrenfreund, P.; Kuan, Y.-J. Spectroscopic diagnostics of organic chemistry in the protostellar environment. *Spectrochimica Acta Part A: Molecular and Biomolecular Spectroscopy* **2001**, *57*, 685−704.

(37) Myers, P. C.; Thaddeus, P.; Linke, R. A. A search for interstellar pyrrole: evidence that rings are less abundant than chains. *Astrophysical Journal* **1980**, *241*, 155−157.

(38) Zhang, L.; Peng, X.-M.; Damu, G. L. V.; Geng, R.-X.; Zhou, C.-H. Comprehensive Review in Current Developments of Imidazole-Based Medicinal Chemistry. *Medicinal Research Reviews* **2014**, *34*, 340−437.

(39) Rosemeyer, H. The Chemodiversity of Purine as a Constituent of Natural Products. *Chemistry & Biodiversity* **2004**, *1*, 361−401.

(40) Dezafra, R. L.; Thaddeus, P.; Kutner, M.; Scoville, N.; Solomon, P. M.; Weaver, H.; Williams, D. R. W. Search for Interstellar Furan and Imidazole. *Astrophys. Lett.* **1971**, *10*, 1−3.

(41) Giuliano, B. M.; Bizzocchi, L.; Pietropolli Charmet, A.; Arenas, B. E.; Steber, A. L.; Schnell, M.; Caselli, P.; Harris, B. J.; Pate, B. H.; Guillemin, J.-C. Rotational spectroscopy of imidazole: improved rest frequencies for astrophysical searches. *Astronomy & Astrophysics* **2019**, *628*, A53.

(42) Vitaku, E.; Smith, D. T.; Njardarson, J. T. Analysis of the Structural Diversity, Substitution Patterns, and Frequency of Nitrogen Heterocycles among U.S. FDA Approved Pharmaceuticals. *J. Med. Chem.* **2014**, *57*, 10257−10274.

(43) Simon, M. N.; Simon, M. Search for Interstellar Acrylonitrile, Pyrimidine, and Pyridine. *Astrophysical Journal* **1973**, *184*, 757−762.

(44) Batchelor, R. A.; Brooks, J. W.; Godfrey, P. D.; Brown, R. D. A Search for Interstellar Molecular Lines in the Frequency Range 8·6 to 9·2 GHz. *Australian Journal of Physics* **1973**, *26*, 557−560.

(45) Charnley, S. B.; Kuan, Y.-J.; Huang, H.-C.; Botta, O.; Butner, H. M.; Cox, N.; Despois, D.; Ehrenfreund, P.; Kisiel, Z.; Lee, Y.-Y.; et al. Astronomical searches for nitrogen heterocycles. *Adv. Space Res.* **2005**, *36*, 137−145.

(46) N, J. B.; Goudgaon, N. M. A comprehensive review on pyrimidine analogs-versatile scaffold with medicinal and biological potential. *J. Mol. Struct.* **2021**, *1246*, 131168.

(47) Irvine, W. M.; Ellder, J.; Hjalmarson, A.; Kollberg, E.; Rydbeck, O. E. H.; Sorensen, G. O.; Bak, B.; Svanholt, H. Searches for interstellar imidazole and cyanoform. *Astronomy & Astrophysics* **1981**, *97*, 192−194.

(48) McGuire, B. A.; Burkhardt, A. M.; Loomis, R. A.; Shingledecker, C. N.; Lee, K. L. K.; Charnley, S. B.; Cordiner, M. A.; Herbst, E.; Kalenskii, S. V.; Momjian, E.; et al. Early science from GOTHAM: Project overview, methods, and the detection of interstellar propargyl cyanide (HCCCH$_2$CN) in TMC-1. *Astrophysical Journal Letters* **2020**, *900*, L10.

(49) Lee, K. L. K.; Patterson, J.; Burkhardt, A. M.; Vankayalapati, V.; McCarthy, M. C.; McGuire, B. A. Machine Learning of Interstellar Chemical Inventories. *Astrophysical Journal Letters* **2021**, *917*, L6.

(50) Thorwirth, S.; Müller, H. S. P.; Winnewisser, G. The Millimeter- and Submillimeter-Wave Spectrum and the Dipole Moment of Ethylenimine. *J. Mol. Spectrosc.* **2000**, *199*, 116−123.

(51) Bogey, M.; Destombes, J.-L.; Denis, J.-M.; Guillemin, J.-C. The millimeter wave rotational spectrum of 2H-azirine, NCH$_2$CH. *J. Mol. Spectrosc.* **1986**, *115*, 1−14.

(52) Hirao, T.; Okabayashi, T.; Tanimoto, M. The r$_0$ Structure of Ethylene Sulfide. *J. Mol. Spectrosc.* **2001**, *208*, 148−149.

(53) Medcraft, C.; Thompson, C. D.; Robertson, E. G.; Appadoo, D. R. T.; McNaughton, D. The far-infrared rotational spectrum of ethylene oxide. *Astrophysical Journal* **2012**, *753*, 18.

(54) Müller, H. S. P.; Guillemin, J.-C.; Lewen, F.; Schlemmer, S. Rotational spectroscopy of isotopic oxirane, c-C$_2$H$_4$O. *J. Mol. Spectrosc.* **2022**, *384*, 111584.

(55) Wlodarczak, G.; Martinache, L.; Demaison, J.; Van Eijck, B. P. The millimeter-wave spectra of furan, pyrrole, and pyridine: Experimental and theoretical determination of the quartic centrifugal distortion constants. *J. Mol. Spectrosc.* **1988**, *127*, 200−208.

(56) Nygaard, U.; Nielsen, J. T.; Kirchheiner, J.; Maltesen, G.; Rastrup-Andersen, J.; Sørensen, G. O. Microwave spectra of isotopic pyrroles. Molecular structure, dipole moment, and ^{14}N quadrupole coupling constants of pyrrole. *J. Mol. Struct.* **1969**, *3*, 491−506.

(57) Orr, V. L.; Ichikawa, Y.; Patel, A. R.; Kougias, S. M.; Kobayashi, K.; Stanton, J. F.; Esselman, B. J.; Woods, R. C.; McMahon, R. J. Precise equilibrium structure determination of thiophene (c-C$_4$H$_4$S) by rotational spectroscopy-Structure of a five-membered heterocycle containing a third-row atom. *J. Chem. Phys.* **2021**, *154*, 244310.

(58) Esselman, B. J.; Zdanovskaia, M. A.; Owen, A. N.; Stanton, J. F.; Woods, R. C.; McMahon, R. J. Precise equilibrium structure of thiazole (c-C$_3$H$_3$NS) from twenty-four isotopologues. *J. Chem. Phys.* **2021**, *155*, 054302.

(59) Kretschmer, U.; Dreizler, H. ^{33}S Nuclear Hyperfine Structure in the Rotational Spectrum of Thiazole. *Zeitschrift für Naturforschung A* **1993**, *48*, 1219−1222.

(60) McCarthy, M. C.; Lee, K. L. K.; Carroll, P. B.; Porterfield, J. P.; Changala, P. B.; Thorpe, J. H.; Stanton, J. F. Exhaustive Product Analysis of Three Benzene Discharges by Microwave Spectroscopy. *J. Phys. Chem. A* **2020**, *124*, 5170−5181.

(61) Esselman, B. J.; Amberger, B. K.; Shutter, J. D.; Daane, M. A.; Stanton, J. F.; Woods, R. C.; McMahon, R. J. Rotational spectroscopy of pyridazine and its isotopologs from 235−360 GHz: Equilibrium structure and vibrational satellites. *J. Chem. Phys.* **2013**, *139*, 224304.

(62) Werner, W.; Dreizler, H.; Rudolph, H. D. Zum Mikrowellenspektrum des Pyridazins. *Zeitschrift für Naturforschung A* **1967**, *22*, 531−543.

(63) Heim, Z. N.; Amberger, B. K.; Esselman, B. J.; Stanton, J. F.; Woods, R. C.; McMahon, R. J. Molecular structure determination: Equilibrium structure of pyrimidine (m-C$_4$H$_4$N$_2$) from rotational spectroscopy (r$_e^{SE}$) and high-level ab initio calculation (r$_e$) agree within the uncertainty of experimental measurement. *J. Chem. Phys.* **2020**, *152*, 104303.

(64) Kisiel, Z.; Pszczółkowski, L.; López, J. C.; Alonso, J. L.; Maris, A.; Caminati, W. Investigation of the Rotational Spectrum of Pyrimidine from 3 to 337 GHz: Molecular Structure, Nuclear Quadrupole Coupling, and Vibrational Satellites. *J. Mol. Spectrosc.* **1999**, *195*, 332−339.

(65) Blackman, G. L.; Brown, R. D.; Burden, F. R. The microwave spectrum, dipole moment, and nuclear quadrupole coupling constants of pyrimidine. *J. Mol. Spectrosc.* **1970**, *35*, 444−454.

(66) Nesvadba, R.; Studecký, T.; Uhlíková, T.; Urban, S. Microwave spectrum and molecular constants of indole. *J. Mol. Spectrosc.* **2017**, *339*, 6−11.

(67) Welzel, A.; Stahl, W. The FT microwave spectrum of benzo[b]thiophene: first application of a new heatable beam nozzle. *Phys. Chem. Chem. Phys.* **1999**, *1*, 5109−5112.

(68) Maris, A.; Michela Giuliano, B.; Melandri, S.; Ottaviani, P.; Caminati, W.; Favero, L. B.; Velino, B. Structure, dipole moment and large amplitude motions of 1-benzofuran. *Phys. Chem. Chem. Phys.* **2005**, *7*, 3317−3322.

(69) Kisiel, Z.; Desyatnyk, O.; Pszczółkowski, L.; Charnley, S. B.; Ehrenfreund, P. Rotational spectra of quinoline and of isoquinoline: spectroscopic constants and electric dipole moments. *J. Mol. Spectrosc.* **2003**, *217*, 115−122.

(70) McNaughton, D.; Godfrey, P. D.; Jahn, M. K.; Dewald, D. A.; Grabow, J.-U. Fourier transform microwave and millimeter wave spectroscopy of quinazoline, quinoxaline, and phthalazine. *J. Chem. Phys.* **2011**, *134*, 154305.

(71) Loomis, R. A.; Öberg, K. I.; Andrews, S. M.; Bergin, E.; Bergner, J.; Blake, G. A.; Cleeves, L. I.; Czekala, I.; Huang, J.; Le Gal, R.; et al. An Unbiased ALMA Spectral Survey of the LkCa 15 and MWC 480 Protoplanetary Disks. *Astrophysical Journal* **2020**, *893*, 101.

(72) Lee, K. L. K.; Loomis, R. A.; Xue, C.; El-Abd, S.; McGuire, B. A. molsim **2021**; DOI: 10.5281/zenodo.5497790.

(73) Foreman-Mackey, D.; Hogg, D. W.; Lang, D.; Goodman, J. emcee: The MCMC Hammer. *Publications of the Astronomical Society of the Pacific* **2013**, *125*, 306−312.

(74) Kumar, R.; Carroll, C.; Hartikainen, A.; Martin, O. ArviZ a unified library for exploratory analysis of Bayesian models in Python. *Journal of Open Source Software* **2019**, *4*, 1143.

(75) Burkhardt, A. M.; Loomis, R. A.; Shingledecker, C. N.; Lee, K. L. K.; Remijan, A. J.; McCarthy, M. C.; McGuire, B. A. Ubiquitous aromatic carbon chemistry at the earliest stages of star formation. *Nature Astronomy* **2021**, *5*, 181−187.

(76) Shingledecker, C. N.; Wandishin, J. T.; Burkhardt, A. M.; Lee, K. L. K.; N, B.; B, C. S.; A, M. B. First Detection of H$_2$CCCHC$_3$N in TMC-1: A Missing Link Between Chains and Rings in Cold Cores? *Astronomy & Astrophysics Letters* **2021**, *652*, L12.

(77) Agúndez, M.; Marcelino, N.; Cabezas, C.; Fuentetaja, R.; Tercero, B.; de Vicente, P.; Cernicharo, J. Detection of the propargyl radical at λ 3 mm. *Astronomy & Astrophysics* **2022**, *657*, A96.

(78) Kaifu, N.; Ohishi, M.; Kawaguchi, K.; Saito, S.; Yamamoto, S.; Miyaji, T.; Miyazawa, K.; Ishikawa, S.-I.; Noumaru, C.; Harasawa, S. A 8.8-50 GHz Complete Spectral Line Survey toward TMC-1 I. Survey Data. *Publications of the Astronomical Society of Japan* **2004**, *56*, 69−173.

(79) Hollis, J. M.; Lovas, F. J.; Remijan, A. J.; Jewell, P. R.; Ilyushin, V. V.; Kleiner, I. Detection of acetamide (CH$_3$CONH$_2$): the largest interstellar molecule with a peptide bond. *Astrophysical Journal* **2006**, *643*, L25.

(80) Chabot, M.; Béroff, K.; Dartois, E.; Pino, T.; Godard, M. Coulomb Explosion of Polycyclic Aromatic Hydrocarbons Induced by Heavy Cosmic Rays: Carbon Chains Production Rates. *Astrophys. J.* **2020**, *888*, 17.

(81) Balucani, N.; Cartechini, L.; Alagia, M.; Casavecchia, P.; Volpi, G. G. Observation of Nitrogen-Bearing Organic Molecules from Reactions of Nitrogen Atoms with Hydrocarbons: A Crossed Beam Study of N(^{2}D) + Ethylene. *J. Phys. Chem. A* **2000**, *104*, 5655−5659.

(82) Turner, A. M.; Chandra, S.; Fortenberry, R. C.; Kaiser, R. I. A Photoionization Reflectron Time-of-Flight Mass Spectrometric Study on the Detection of Ethynamine (HCCNH$_2$) and 2H-Azirine (c-H$_2$CCHN). *ChemPhysChem* **2021**, *22*, 985−994.

(83) Occhiogrosso, A.; Vasyunin, A.; Herbst, E.; Viti, S.; Ward, M. D.; Price, S. D.; Brown, W. A. Ethylene oxide and acetaldehyde in hot cores. *Astronomy & Astrophysics* **2014**, *564*, A123.

(84) Bennett, C. J.; Osamura, Y.; Lebar, M. D.; Kaiser, R. I. Laboratory Studies on the Formation of Three C$_2$H$_4$O Isomers-Acetaldehyde (CH$_3$CHO), Ethylene Oxide (c-C$_2$H$_4$O), and Vinyl Alcohol (CH$_2$CHOH)-in Interstellar and Cometary Ices. *Astrophysical Journal* **2005**, *634*, 698−711.

(85) Bergner, J. B.; Öberg, K. I.; Rajappan, M. Oxygen Atom Reactions with C$_2$H$_6$, C$_2$H$_4$, and C$_2$H$_2$ in Ices. *Astrophysical Journal* **2019**, *874*, 115.

(86) Balucani, N. Elementary Reactions and Their Role in Gas-Phase Prebiotic Chemistry. *International Journal of Molecular Sciences* **2009**, *10*, 2304−2335.

(87) Leonori, F.; Petrucci, R.; Balucani, N.; Casavecchia, P.; Rosi, M.; Skouteris, D.; Berteloite, C.; Le Picard, S. D.; Canosa, A.; Sims, I. R. Crossed-Beam Dynamics, Low-Temperature Kinetics, and Theoretical Studies of the Reaction S(^{1}D) + C$_2$H$_4$. *J. Phys. Chem. A* **2009**, *113*, 15328−15345.

(88) Lockyear, J. F.; Welz, O.; Savee, J. D.; Goulay, F.; Trevitt, A. J.; Taatjes, C. A.; Osborn, D. L.; Leone, S. R. Isomer Specific Product Detection in the Reaction of CH with Acrolein. *J. Phys. Chem. A* **2013**, *117*, 11013−11026.

(89) Tuazon, E. C.; Alvarado, A.; Aschmann, S. M.; Atkinson, R.; Arey, J. Products of the Gas-Phase Reactions of 1,3-Butadiene with OH and NO$_3$ Radicals. *Environ. Sci. Technol.* **1999**, *33*, 3586−3595.

(90) Ricca, A.; Bauschlicher, C. W.; Bakes, E. L. O. A Computational Study of the Mechanisms for the Incorporation of a Nitrogen Atom into Polycyclic Aromatic Hydrocarbons in the Titan Haze. *Icarus* **2001**, *154*, 516−521.

(91) Hamid, A. M.; Bera, P. P.; Lee, T. J.; Aziz, S. G.; Alyoubi, A. O.; El-Shall, M. S. Evidence for the Formation of Pyrimidine Cations from the Sequential Reactions of Hydrogen Cyanide with the Acetylene Radical Cation. *J. Phys. Chem. Lett.* **2014**, *5*, 3392−3398.

(92) Stein, T.; Bera, P. P.; Lee, T. J.; Head-Gordon, M. Molecular growth upon ionization of van der Waals clusters containing HCCH and HCN is a pathway to prebiotic molecules. *Phys. Chem. Chem. Phys.* **2020**, *22*, 20337−20348.

(93) Soorkia, S.; Taatjes, C. A.; Osborn, D. L.; Selby, T. M.; Trevitt, A. J.; Wilson, K. R.; Leone, S. R. Direct detection of pyridine formation by the reaction of CH (CD) with pyrrole: a ring expansion reaction. *Phys. Chem. Chem. Phys.* **2010**, *12*, 8750−8758.

(94) Morales, S. B.; Bennett, C. J.; Le Picard, S. D.; Canosa, A.; Sims, I. R.; Sun, B. J.; Chen, P. H.; Chang, A. H. H.; Kislov, V. V.; Mebel, A. M.; et al. A crossed molecular beam, low-temperature kinetics, and theoretical investigation of the reaction of the cyano radical (CN) with 1,3-butadiene (C$_4$H$_6$). A route to complex nitrogen-bearing molecules in low-temperature extraterrestrial environments. *Astrophysical Journal* **2011**, *742*, 26−10.

(95) Parker, D. S. N.; Kaiser, R. I.; Kostko, O.; Troy, T. P.; Ahmed, M.; Sun, B.-J.; Chen, S.-H.; Chang, A. H. H. On the formation of pyridine in the interstellar medium. *Phys. Chem. Chem. Phys.* **2015**, *17*, 32000−32008.

(96) Fondren, L. D.; McLain, J.; Jackson, D. M.; Adams, N. G.; Babcock, L. M. Studies of reactions of a series of ions with nitrogen containing heterocyclic molecules using a selected ion flow tube. *Int. J. Mass Spectrom.* **2007**, *265*, 60−67.

(97) Balucani, N.; Pacifici, L.; Skouteris, D.; Caracciolo, A.; Casavecchia, P.; Falcinelli, S.; Rosi, M. A Computational Study of the Reaction N(^{2}D)+C$_6$H$_6$ Leading to Pyridine and Phenylnitrene. *Computational Science and Its Applications - ICCSA 2019*; ICCSA, 2019; pp 316−324.

(98) Chin, C.-H.; Zhu, T.; Zhang, J. Z. H. Cyclopentadienyl radical formation from the reaction of excited nitrogen atoms with benzene: a theoretical study. *Phys. Chem. Chem. Phys.* **2021**, *23*, 12408−12420.

(99) Krasnopolsky, V. A. A photochemical model of Titanas atmosphere and ionosphere. *Icarus* **2009**, *201*, 226−256.

(100) Loison, J. C.; Hébrard, E.; Dobrijevic, M.; Hickson, K. M.; Caralp, F.; Hue, V.; Gronoff, G.; Venot, O.; Bénilan, Y. The neutral photochemistry of nitriles, amines and imines in the atmosphere of Titan. *Icarus* **2015**, *247*, 218−247.

(101) Materese, C. K.; Nuevo, M.; Sandford, S. A. N- and O-heterocycles Produced From The Irradiation Of Benzene And Naphthalene In H$_2$O/NH$_3$-containing Ices. *Astrophysical Journal* **2015**, *800*, 116.

(102) Parker, D. S. N.; Kaiser, R. I.; Kostko, O.; Troy, T. P.; Ahmed, M.; Mebel, A. M.; Tielens, A. G. G. M. Gas phase synthesis of (iso)quinoline and its role in the formation of nucleobases in the interstellar medium. *Astrophysical Journal* **2015**, *803*, 53.

(103) Lin, M.-F.; Dyakov, Y. A.; Tseng, C.-M.; Mebel, A. M.; Hsien Lin, S.; Lee, Y. T.; Ni, C.-K. Photodissociation dynamics of pyridine. *J. Chem. Phys.* **2005**, *123*, 054309.

(104) Parker, D. S. N.; Yang, T.; Dangi, B. B.; Kaiser, R. I.; Bera, P. P.; Lee, T. J. Low temperature formation of nitrogen-substituted polycyclic aromatic hydrocarbons (PANHs)-barrierless routes to dihydro(iso)quinolines. *Astrophysical Journal* **2015**, *815*, 115.

(105) Oba, Y.; Takano, Y.; Naraoka, H.; Watanabe, N.; Kouchi, A. Nucleobase synthesis in interstellar ices. *Nat. Commun.* **2019**, *10*, 4413.

(106) Peeters, Z.; Botta, O.; Charnley, S. B.; Kisiel, Z.; Kuan, Y.-J.; Ehrenfreund, P. Formation and photostability of N-heterocycles in space. *Astronomy & Astrophysics* **2005**, *433*, 583−590.

(107) Lee, K. L. K.; McCarthy, M. Study of Benzene Fragmentation, Isomerization, and Growth Using Microwave Spectroscopy. *J. Phys. Chem. Lett.* **2019**, *10*, 2408−2413.

(108) Cooke, I. R.; Gupta, D.; Messinger, J. P.; Sims, I. R. Benzonitrile as a proxy for benzene in the cold ISM: low temperature rate coefficients for CN + C$_6$H$_6$. *Astrophysical Journal Letters* **2020**, *891*, L41.

(109) Miksch, A. M.; Riffelt, A.; Oliveira, R.; Kästner, J.; Molpeceres, G. Hydrogenation of small aromatic heterocycles at low temperatures. *Mon. Not. R. Astron. Soc.* **2021**, *505*, 3157−3164.

(110) Sims, I. R.; Queffelec, J.-L.; Travers, D.; Rowe, B. R.; Herbert, L. B.; Karthäuser, J.; Smith, I. W. Rate constants for the reactions of CN with hydrocarbons at low and ultra-low temperatures. *Chem. Phys. Lett.* **1993**, *211*, 461−468.

(111) Chastaing, D.; James, P. L.; Sims, I. R.; Smith, I. W. M. Neutral−neutral reactions at the temperatures of interstellar clouds Rate coefficients for reactions of C_2H radicals with O_2, C_2H_2, C_2H_4 and C_3H_6 down to 15 K. *Faraday Discuss.* **1998**, *109*, 165−181.

(112) Fortenberry, R. C. The Formation of Astromolecule Ethynyl Cyclopropenylidene (c-C_3HCCH) from C_2H and c-C_3H_2. *Astrophysical Journal* **2021**, *921*, 132.

(113) Goulay, F.; Leone, S. R. Low-Temperature Rate Coefficients for the Reaction of Ethynyl Radical (C_2H) with Benzene. *J. Phys. Chem. A* **2006**, *110*, 1875−1880.

🕮 Recommended by ACS

Infrared Spectra and Intensities of Amorphous and Crystalline Allene

Reggie L. Hudson and Yukiko Y. Yarnall

APRIL 19, 2022
ACS EARTH AND SPACE CHEMISTRY   READ 🗗

Far-IR Absorption of Neutral Polycyclic Aromatic Hydrocarbons (PAHs): Light on the Mechanism of IR–UV Ion Dip Spectroscopy

Alexander K. Lemmens, Anouk M. Rijs, *et al.*

OCTOBER 09, 2020
THE JOURNAL OF PHYSICAL CHEMISTRY LETTERS   READ 🗗

Aromatics and Cyclic Molecules in Molecular Clouds: A New Dimension of Interstellar Organic Chemistry

Michael C. McCarthy and Brett A. McGuire

MARCH 22, 2021
THE JOURNAL OF PHYSICAL CHEMISTRY A   READ 🗗

Chirped-Pulse Fourier Transform Millimeter-Wave Spectroscopy of Furan, Isotopologues, and Vibrational Excited States

Timothy J. Barnum, Brett A. McGuire, *et al.*

OCTOBER 20, 2021
ACS EARTH AND SPACE CHEMISTRY   READ 🗗

Get More Suggestions >